SEMIKRON
innovation+service

Application Note
AN1401

Revision:	02
Issue date:	2015-06-03
Prepared by:	Niklas Hofstötter
Approved by:	Peter Beckedahl

Keyword: IGBT, switch, turn, Miller, parasitic, unipolar, Gate, supply, voltage, positive, negative

Limits and hints how to turn off IGBTs with unipolar supply

Equipment manufacturers in the field of power electronics attempt to offer their products, such as electric drives, inverters for solar systems or UPSs in the most cost effective and space saving manner. For this reason, when driving modules in the low power range, they often resort to driving the power semiconductors with 0V (unipolar), instead of the usual negative turn-off voltage such as -8V to -15V (bipolar).

This application note is to point out the problems and limitations of unipolar driving of IGBTs and serves as an aid to the correct operation of unipolar controlled IGBTs.

1. Risks in Turning Off IGBTs with 0V

Unipolar switching of IGBTs, in contrast to bipolar switching, decreases the gap between the gate turn-off voltage of the driver and the threshold voltage $V_{GE(th)}$ of the IGBT, at which it changes into the conductive state. Typical datasheet values for the threshold voltage are in the range of about 5V to 6.5V at a chip temperature of 25°C. With increasing chip temperature the threshold voltage decreases by a few mV/K.

The small gap between the gate turn-off voltage and the threshold voltage of the IGBT increases the risk of parasitic turn-on of the IGBTs. Parasitic switching can be caused by the feedback effect of the Miller capacitance or by the influence of the parasitic inductance in the emitter branch. These two cases will be explained in more detail later. If an IGBT turns on parasitically, a current may flow in the phase leg, which creates additional losses in both of the IGBTs in question.

In addition to parasitic switching, consideration should be given to the fact that, when driving IGBTs unipolar, the switching delay times change, and, depending on the IGBT chip generation and technology, so will the switching losses.

1.1 Parasitic inductances

All power modules suffer from parasitic inductances which exist due to the power terminals and the internal chip connections. Especially in fast-switching modules this leads to over-voltages across IGBTs and diodes. The presence of parasitic inductances in current paths shared by both the load circuit and the control circuit (gate circuit), will influence the IGBT's gate-emitter voltage $V_{GE'}$ when switching the load current.

Figure 1 shows an IGBT with an inverse diode, and the parasitic inductance in the gate-emitter path. For simplicity, only one inductance is shown. In practice, this is a complex system of self-inductance and coupled inductances of the power and control circuit.

Figure 1: Switch with parasitic inductance in the gate-emitter path

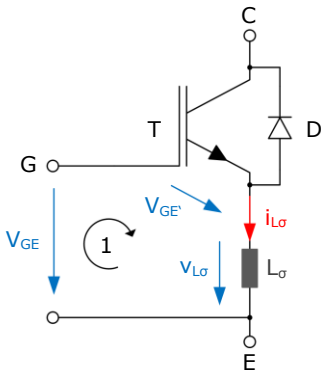

When the load current changes in the parasitic inductance, a voltage will build up across the inductor due to the self-induction. A positive change in current induces a positive voltage, a negative change in current results in a negative voltage. The value of the induced voltage is calculated according to the equation of Faraday's Law.

$$v_{L\sigma} = L_\sigma \cdot \frac{di_{L\sigma}}{dt}$$

A positive induction voltage reduces the gate-emitter voltage $V_{GE'}$ according to the mesh equation ① (see arrow in Figure 1), a negative induction voltage increases the gate-emitter voltage.

$$V_{GE'} = V_{GE} - v_{L\sigma}$$

Both, turning on and off the IGBT T as well as switching of the diode D causes a change in current in the parasitic inductance L_σ.

Figure 2 shows the block diagram of one phase leg with the parasitic inductances in the gate-emitter circuit (left), as well as the current and voltage waveforms of the parasitic inductance $L_{\sigma 2}$ when switching on and off IGBT T_2 and diode D_2.

Figure 2: Block diagram of one phase with the parasitic inductances in the gate-emitter circuit

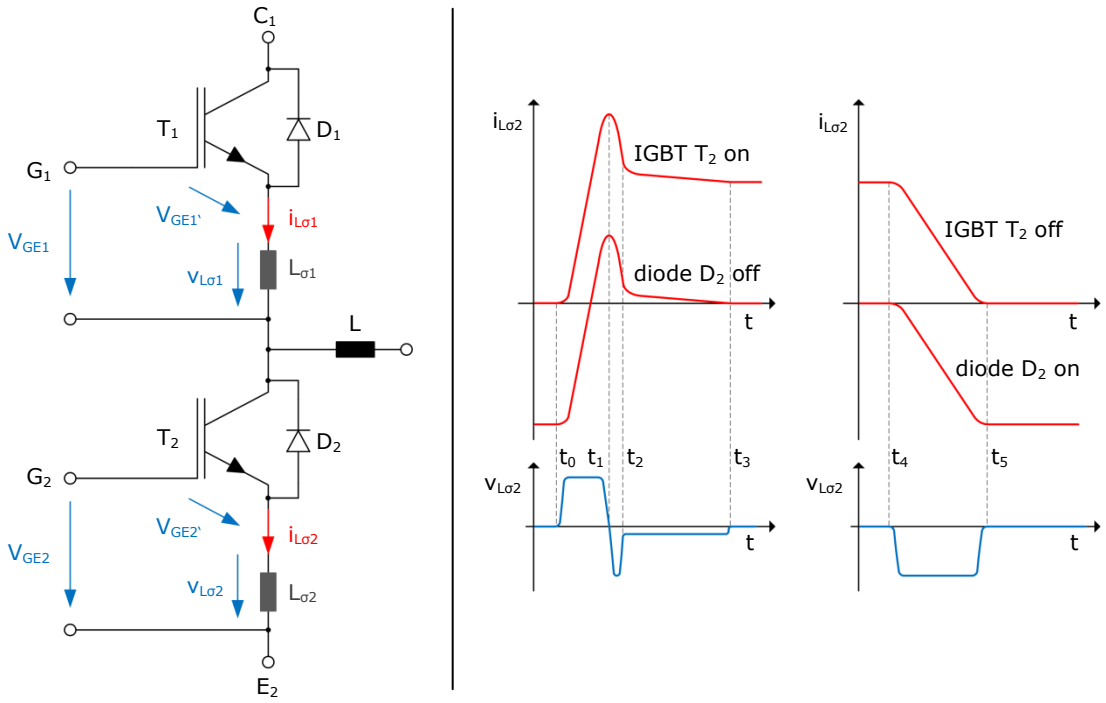

When IGBT T_2 is turned on, the load current of the diode D_1 commutates to IGBT T_2. Until the peak of the reverse current (t_0 - t_1) a positive voltage is induced across the parasitic inductance $L_{\sigma 2}$, reducing the gate-emitter voltage $V_{GE2'}$. During the decay phase of the reverse current peak of diode D_2 (t_1 - t_3), the induced voltage across the parasitic inductance $L_{\sigma 2}$ is negative, thus the gate-emitter voltage $V_{GE2'}$ increases. When turning off IGBT T_2, the load current of IGBT T_2 commutates to diode D_1. The hereby induced voltage in the parasitic inductance $L_{\sigma 2}$ raises the gate-emitter voltage $V_{GE2'}$ from the time t_4 to time t_5. Both cases introduce a negative feedback for the IGBT that slows the switching and, therefore, the switching losses increase. As a positive side effect this provides better controllability of a short-circuit situation [2].

When the complementary IGBT T_1 is turned off, the diode D_2 turns on and takes over the load current of IGBT T_1. From the time t_4 to time t_5 the induced voltage $v_{L\sigma 2}$ increases the gate-emitter voltage of IGBT T_2. A parasitic turn-on of IGBT T_2 during this period is not a problem, because the current already flows in the other direction through the parallel diode D_2.

Critical, however, is the time of turn-on of the complementary IGBT T_1 in which the load current of the diode D_2 commutates to IGBT T_1. During the decay phase of the reverse current of diode D_2, from time t_1 to t_3, the gate-emitter voltage of IGBT T_2 is raised. If this reaches the value of the threshold voltage, IGBT T_2 turns on and a cross-current flows in the phase leg, causing additional losses in T_1 and T_2.

1.2 Effect of the Miller capacitance

The Miller capacitance C_{GC} exists due to the internal structure of the IGBT, and, in the equivalent circuit, consists of two individual capacitances arranged in series. The first capacitance, which forms due to the oxide layer of the gate, has a constant value. The value of the second capacitance varies with the width of the space-charge zone in the n^--drift region, and is thus dependent on the collector-emitter voltage. Any change in the collector-emitter voltage causes a displacement current through the Miller capacitance.

Figure 3: Displacement current due to the Miller capacitance

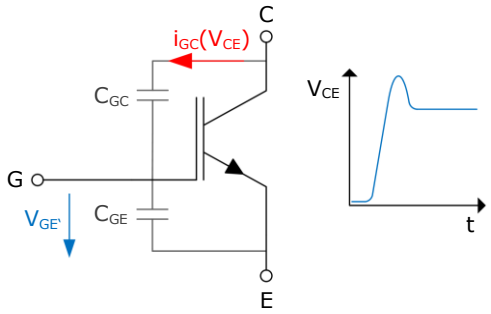

The value of the current is calculated approximately from the product of the magnitude of the Miller capacitance and the rate of change of the collector-emitter voltage.

$$i_{GC}(V_{CE}) = C_{GC}(V_{CE}) \cdot \frac{dv_{CE}}{dt}$$

The displacement current i_{GC} increases the voltage at the on-chip gate-emitter capacitance and thus the gate-emitter voltage $V_{GE'}$ of the IGBT. The amplitude of the voltage depends on the capacitive voltage divider of the internal semiconductor capacitances C_{GC} and C_{GE}, the internal gate resistance R_{Gint}, and the gate's external circuitry. Once the gate-emitter voltage $V_{GE'}$ reaches the threshold voltage, the IGBT begins to change into the conductive state. A cross-current begins to flow in the phase leg, causing additional losses in both the IGBTs of the bridge leg concerned. (This phenomenon is also known as Miller-induced shoot-through.)

The cross-current results in a change of the current increase in the parasitic inductances of the load circuit. Due to the self-induction the parasitic inductances take over part of the DC-bus voltage and reduce the rate of change of the collector-emitter voltage. An equilibrium arises between the degree of IGBT turn-on and the feedback of the Miller capacitance on the gate circuit. This causes the value of the gate-emitter voltage not to increase much further than the value of the threshold voltage of the IGBT.

Neglecting the parasitic inductances in the gate circuit it reduces the equivalent circuit diagram of the feedback circuit to the RC-network shown in Figure 4.

Figure 4: Equivalent circuit diagram of the gate circuit

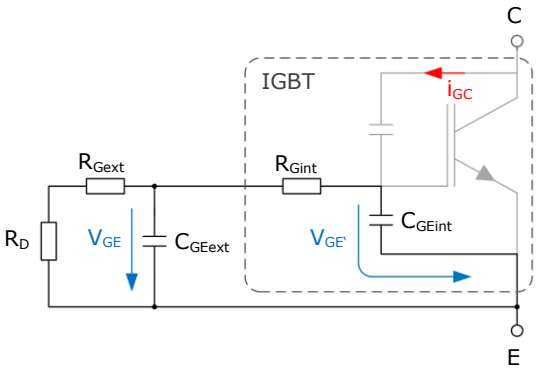

Once the IGBT is in steady state and the change of the collector-emitter voltage is constant, the gate-emitter voltage $V_{GE'}$ caused by the displacement current depends on the sum of the gate resistor values and the internal driver resistance $(R_{ges} = R_{Gext} + R_{Gint} + R_D)$. The larger the summed resistance, the larger the gate-emitter voltage $(V_{GE'} = R_{ges} \cdot i_{GC})$. The gate-emitter voltage time function is determined by the time constant of the RC-network connected. The larger the capacitances of the network, the longer it takes for the steady state to arrive.

2. Measurements with the MiniSKiiP®24NAB12T4V1

The MiniSKiiP®24NAB12T4V1 is a 35A module consisting of a rectifier, a brake chopper and an inverter unit. The following investigations were carried out on one phase leg of the inverter. A phase leg consists of two series-connected IGBTs and the associated freewheeling diodes. The upper switch is referred to as TOP IGBT the lower as BOT IGBT. This module uses 1200V IGBT Trench 4 chips without internal gate resistor, and CAL4 freewheeling diodes.

Figure 5: Equivalent circuit diagram of the gate circuit

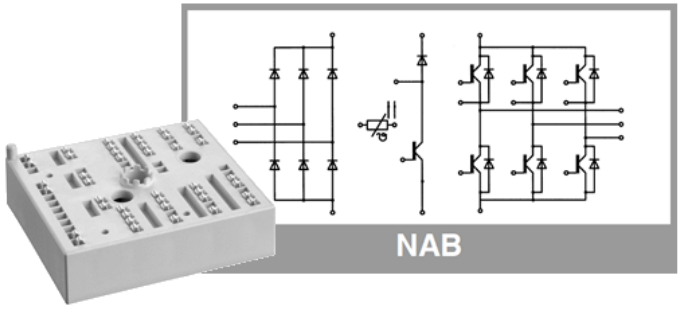

To determine the dynamic characteristics a double pulse method was used with an inductive load. Figure 6 shows the basic configuration for measuring the TOP IGBT (right) or BOT IGBT (left). Depending on requirements, either the TOP or BOT IGBT is switched, while the inactive IGBT is kept in the off-state by the driver.

Figure 6: Block diagram of the double-pulse test

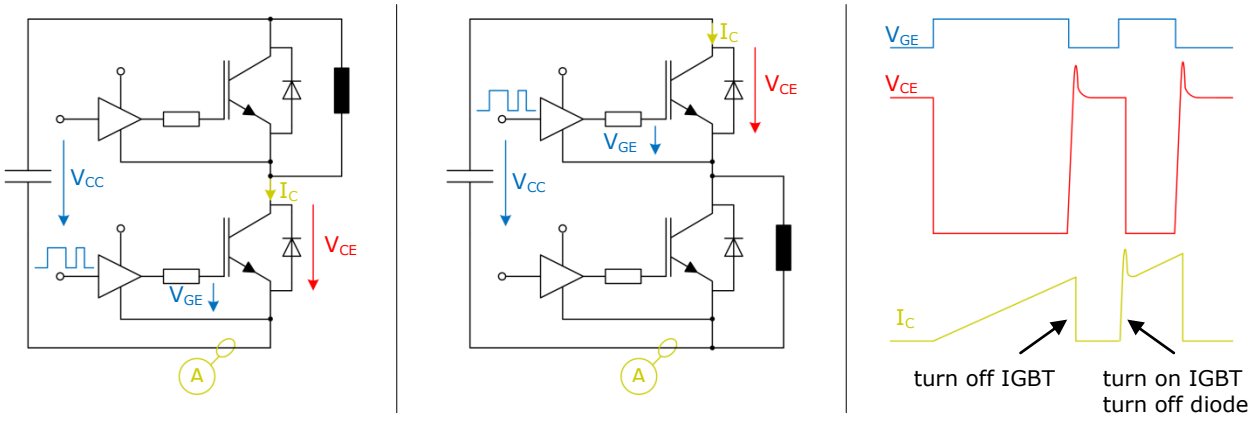

2.1 Comparative measurements of the dynamic switching behavior with bipolar and unipolar gate drive

In order to compare the dynamic behaviour of an IGBT with bipolar and with unipolar control, the dynamic characteristics of both types of control were determined on the same IGBT using a double pulse method. First, the dynamic behaviour of the IGBT has been studied with bipolar drive. Afterwards, the driver was modified so that it could be used for the measurement with unipolar drive. Both measurements were carried out under identical conditions, apart from the gate-emitter voltage.

Table 1: Measurements on the MiniSKiiP®24NAB12T4V1

		V_{CC}	=	600V	
		T_j	=	150°C	
		R_{Gon}	=	18Ω	
		R_{Goff}	=	18Ω	
		I_C	=	35A	
bipolar				unipolar	
V_{GE}	=	±15V		V_{GE}	= 0/15V
E_{on}	=	100%		E_{on}	= 102%
E_{off}	=	100%		E_{off}	= 104%
$t_{d(on)}$*	=	133ns		$t_{d(on)}$*	= 57ns
$t_{d(off)}$*	=	345ns		$t_{d(off)}$*	= 476ns

* Definition of $t_{d(on)}$ and $t_{d(off)}$ according to Figure 7.

Figure 7 shows the switching behaviour of an IGBT with bipolar control (top) compared with the switching behaviour with unipolar control (bottom).

Figure 7: Turn-on and turn-off behaviour with bipolar and unipolar control

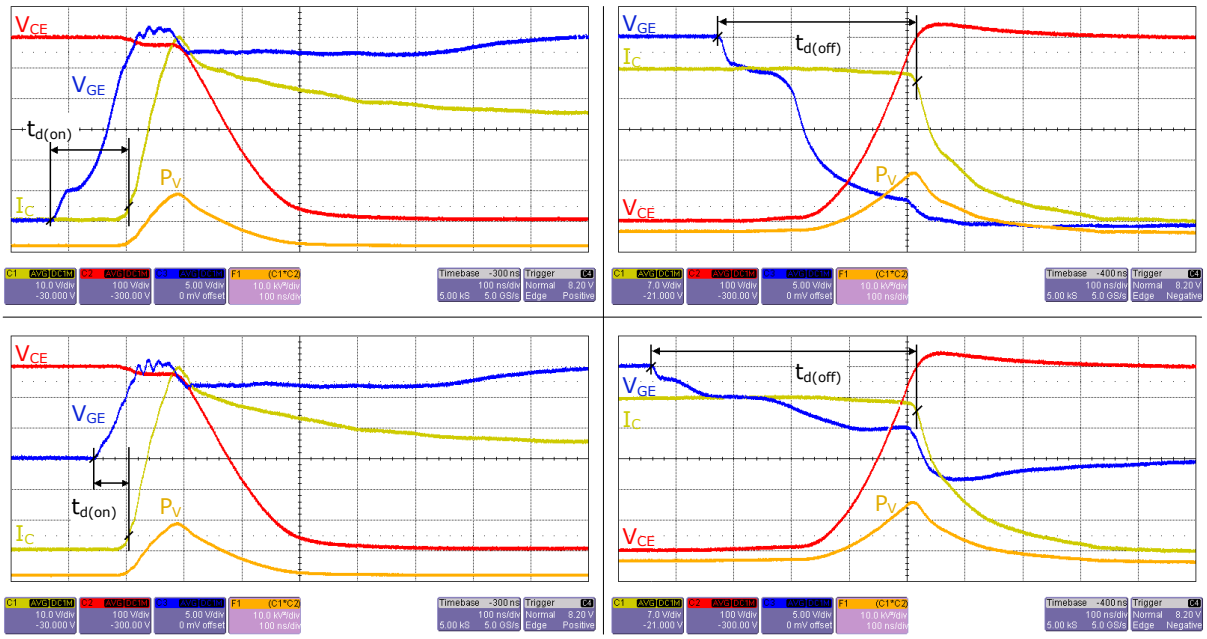

Comparing the waveforms of the unipolar driven IGBT with those of the bipolar driven IGBT, it can be observed that both curves of the collector currents and of the collector-emitter voltages are almost identical, both at turn-on and turn-off. Since current and voltage waveforms differ only slightly from each other, the calculated energy dissipations remain at a similar level as well.

The reason for the almost identical turn-on losses is easily explained. Upon reaching the threshold voltage, the actual switching of the IGBT begins. The speed of the switching operation depends on the charging of the internal semiconductor capacitances and thus on the amount of charge carriers that may be brought into the gate within a certain period. Since the driving voltage during turn-on, which is measured from the threshold voltage to the full gate turn-on voltage of the driver, is the same in the two control modes, the switching losses are also similiar.

The reason for the almost identical turn-off losses originates in the turn-off behaviour of the 1200V IGBT Trench 4. If an IGBT is turned off with 0V instead of a negative voltage, then, with the same gate resistance, a smaller gate current flows, discharging the internal semiconductor capacitance. A minimization of the gate current can be achieved with the same gate voltage also by an increase in the gate resistance. Thus, the unipolar switching is similar in consequence to an increase in the gate resistance. The seeming increase in the resistance value can be determined in a good approximation with the following formula.

$$R_{G'} = R_G \cdot \frac{V_{GE(th)} - V_{G(off\ bipolar)}}{V_{GE(th)}}$$

As can be seen in Figure 8, the energy dissipations, when switching off the 1200V IGBT Trench 4, are nearly constant over a wide range of the gate resistance value. As long as the calculated value for $R_{G'}$ is in the constant region of the energy dissipation characteristic, only small differences in energy dissipation between the unipolar and bipolar switching can be expected.

Figure 8: Switching energy dissipations in the MiniSKiiP®24NAB12T4V1

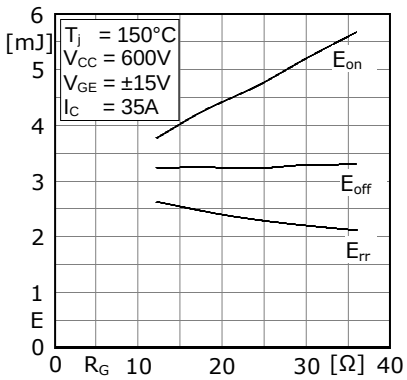

For other IGBT generations and technologies for which there is a relation $E_{off} = f(R_G)$, increased turn-off losses have been demonstrated in unipolar switching. The amount of change can be estimated via the gate resistor analogy from the above formula.

Differences can be observed for the turn-on and turn-off delay times. As can be seen in Figure 7 the delay time increases for turn-off and decreases when turning on. This must be taken into account when setting the interlock times.

2.2 Turn-Off of the inverse diode

The following measurements are used to consider the influence of the Miller capacitance and the parasitic emitter inductance on the gate circuit of the turned off IGBT T_2, when switching the complimentary IGBT T_1. Figure 9 shows the block diagram of this measurement set-up. To enable the measurement of the gate-emitter voltage $V_{GE'}$ and the induced voltage $v_{L\sigma 2}$, an additional sense wire is attached directly to the emitter of IGBT T_2. Gate resistors were those shown in the datasheet; 18Ω for both turning on and off of the IGBTs.

Figure 9: Block diagram of the measurements on the MiniSKiiP®24NAB12T4V1

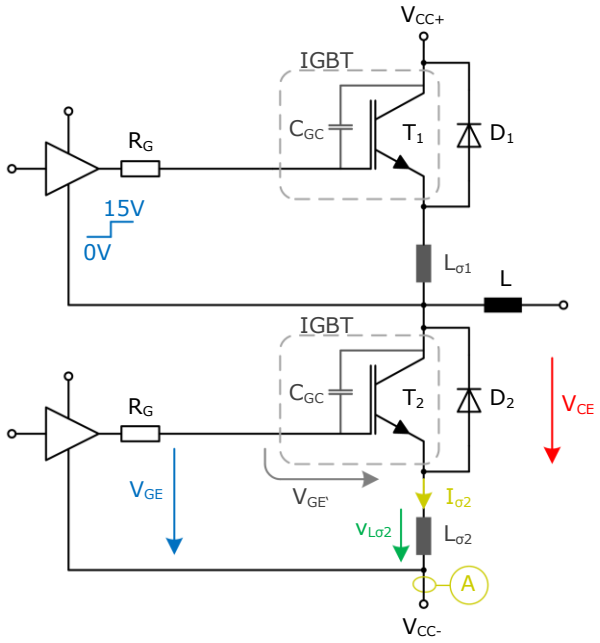

Figure 10 shows the curves measured on IGBT T_2 and diode D_2 upon turn-on of the complementary IGBT T_1. When T_1 turns on, the current commutates from the freewheeling diode D_2 to IGBT T_1. The commutation speed depends on the switching speed of IGBT T_1 and the commutation inductance.

From the beginning of the current commutation to the maximum of the reverse current of the diode, the parasitic inductance $L_{\sigma 2}$ is the main factor influencing the gate-emitter voltage $V_{GE'}$ of IGBT T_2. Since, during this time, the $di_{L\sigma 2}/dt$ is positive, the gate-emitter voltage $V_{GE'}$ is negative, and the IGBT remains turned off safely.

The critical period starts with the decay of the reverse current, as the change in current through the parasitic inductance is negative here. As a result, the gate-emitter voltage of IGBT T_2 is raised. This effect is superimposed by the effect of the Miller capacitance, since diode D_2 starts to pick up off-state (reverse) voltage. With the building up of the reverse voltage, the collector-emitter voltage increases across IGBT T_2, which in turn causes a displacement current through the Miller capacitance in the direction of the driver. This displacement current additionally raises the gate-emitter voltage of IGBT T_2.

Once the tail current phase is reached the influence of the parasitic inductance decreases, because the rate of change of the current decreases. The gate-emitter voltage of IGBT T_2 decreases slightly then, but is held up due to the effect of the Miller capacitance, until diode D_2 has completely built up its reverse voltage.

The measurements on the MiniSKiiP®24NAB12T4V1 show that without the additionally attached sense wire, the real voltage across the chip cannot be measured, as long as the effect of the parasitic inductance is affecting the gate-emitter voltage. Once the tail current phase is reached both measured voltages V_{GE} and $V_{GE'}$ are nearly identical and it can be assumed that the measured voltage at the module connection is relatively close to the actual voltage value.

The curves also show that the gate-emitter voltage $V_{GE'}$ on the turned off IGBT T_2 reaches the critical level of the threshold voltage $V_{GE(th)}$, but a parasitic turn-on cannot be observed.

Figure 10: Turn-off of the inverse diode with R_G = 18Ω and C_{GE} = 0nF

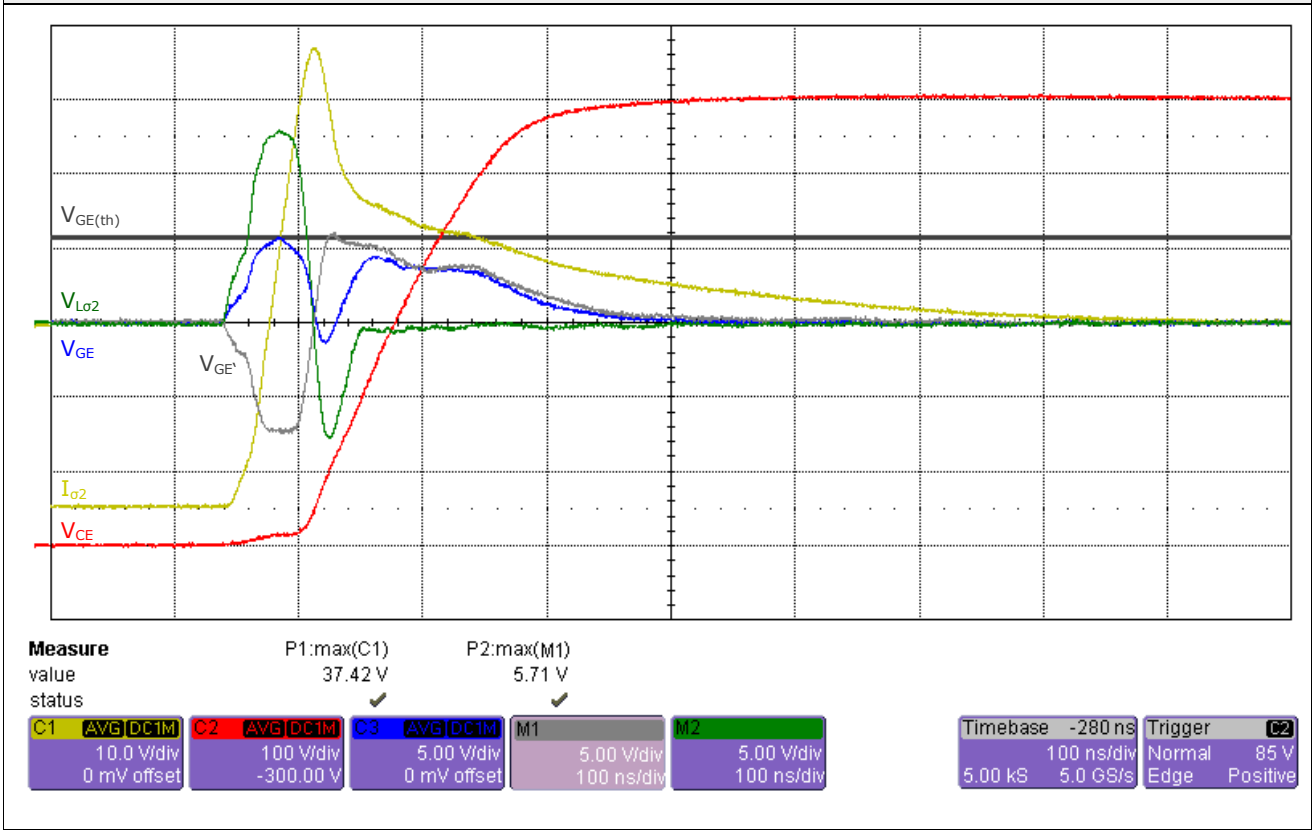

2.3 Reduction of the parasitic effects with additional gate-emitter capacitance

For this measurement, external gate-emitter capacitance, each with a value of 10nF, has been added at IGBT T_1 and T_2. The selected external gate-emitter capacitance is about five times greater than the value of the input capacitance Cies of the IGBTs. The influence of the Miller capacitance and the parasitic inductance was again measured in the gate circuit. Again, the turn-off of the diode D_2 was considered during the turn-on of the complementary IGBT T_1. Since the external gate-emitter capacitance slows down the switching behaviour of the IGBT, smaller gate resistors of 6.2Ω were used to compensate.

Figure 11 shows the block diagram of the measurement setup.

Figure 11: Block diagram of the measurements on the MiniSKiiP®24NAB12T4V1 with external gate-emitter capacitance

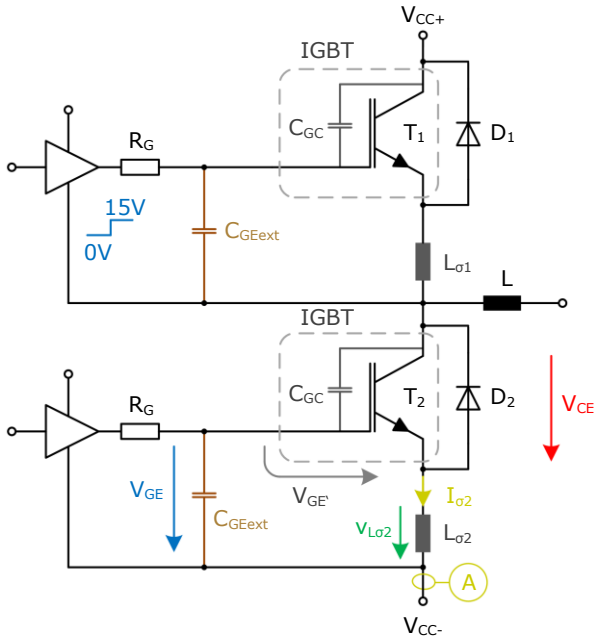

Figure 12 shows the commutation of the current from diode D_2 to IGBT T_1. If compared to the previous measurement (Figure 10) the voltage profiles show a significant reduction of parasitic influences.

On the one hand the influence of the Miller capacitance is reduced by the use of the external gate-emitter capacitance on IGBT T_2. The external capacitor increases the total capacitance between the gate and the emitter. Hence, there are more charge carriers needed to bring the gate-emitter voltage $V_{GE'}$ into the region of the threshold voltage $V_{GE(th)}$.

On the other hand, the influence of the parasitic inductance is reduced by the use of the external gate-emitter capacitance at IGBT T_1. The external capacitance slows down the turn-on of IGBT T_1 and hence the commutation of the current of the freewheeling diode D_2 to IGBT T_1. The reduction of the current rate of change by the parasitic inductances minimizes the induced voltage in the gate circuit. The gate-emitter voltage of IGBT T_2 is therefore not increased as much.

Further, the smaller gate turn-off resistor (R_{Goff} = 6.2Ω) reduces the parallel impedance to deal with the capacitive displacement current and it also reduces the influence of the Miller capacitance for the gate circuit.

In order to prevent parasitic switching of an IGBT, it is recommended that the external gate-emitter capacitance be selected so that the value of the gate-emitter voltage does not exceed half of the threshold voltage (2.5V to 3V).

Figure 12: Turn-off of the inverse diode with R_G = 6.2Ω and C_{GE} = 10nF

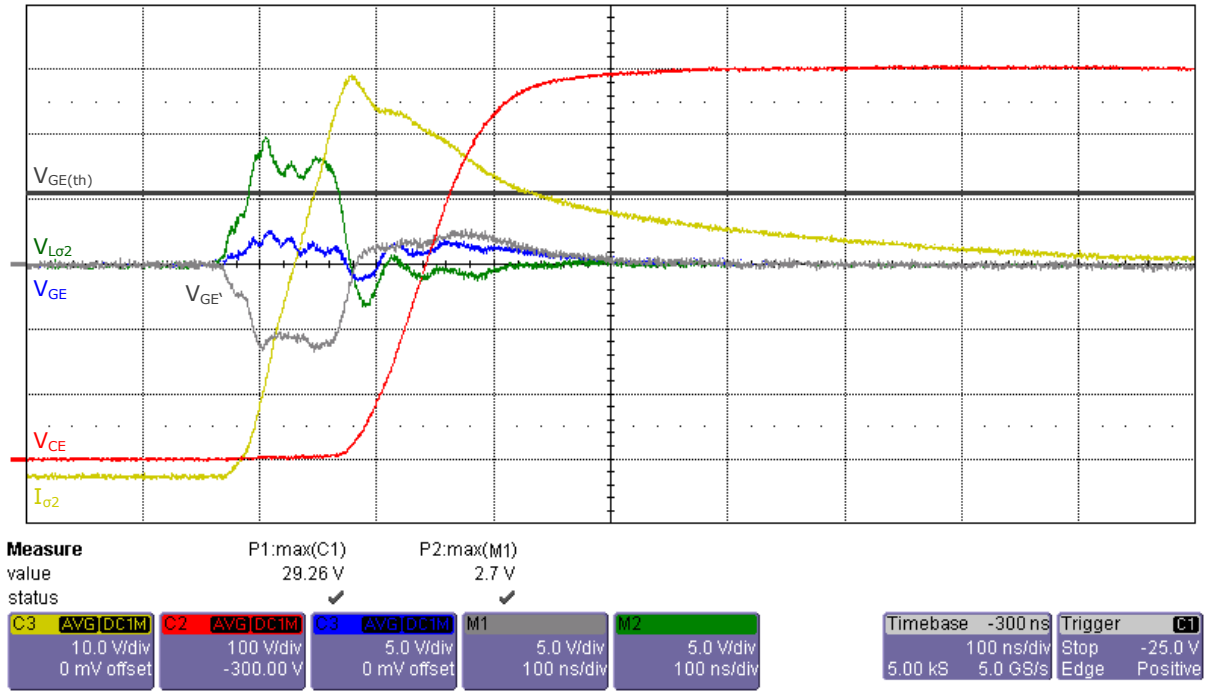

2.4 Influence of the external gate-emitter capacitance on the switching Losses

The positive properties of the external gate-emitter capacitance, with which the parasitic effects are minimised, have the disadvantage of an increase in switching losses, as the additional gate-emitter capacitance of the IGBT slows down the switching process. Another disadvantage is the additional driving power ($P = f_{sw} \cdot C_{GEext} \cdot \Delta V^2$) required to change the charge of the external gate-emitter capacitance.

In order to minimise the switching losses in spite of an external gate-emitter capacitance, the value of the gate resistor can be adjusted. It must be noted, however, that any change in the value of the gate resistors requires a new SOA-calculation as well as a fresh investigation of the parasitic effects.

In the present case the MiniSKiiP®24NAB12T4V1 could be operated with a resistance value (R_{Gon}, R_{Goff}) of 6.2Ω and an external gate-emitter capacitance of 10nF. Table 2 shows the switching losses as a function of the resistor values and the value of the external gate-emitter capacitor. The values of the switching losses are given in percent. One hundred percent corresponds to the data sheet value.

Table 2: Relative switching losses of the MiniSKiiP®24NAB12T4V1 with different gate resistors and gate-emitter capacitances

	E_{off} [%]		E_{on} [%]		E_{off} + E_{on} [%]	
	R_G = 18Ω	R_G = 6.2Ω	R_G = 18Ω	R_G = 6.2Ω	R_G = 18Ω	R_G = 6.2Ω
0.0nF	100.0	96.5	100.0	75.4	100.0	84.1
1.0nF	100.6	97.1	101.0	74.8	100.8	84.0
4.7nF	100.9	97.1	112.3	75.8	107.6	84.6
10.0nF	102.9	97.4	134.8	84.2	121.7	89.7
15.0nF	106.1	98.0	152.5	92.8	133.3	94.9

3. Measurements and Simulation with the MiniSKiiP®39AC12T4V1

The MiniSKiiP®39AC12T4V1 is a 150A inverter module. The following study is carried out on one phase leg of the inverter. A phase leg consists of two switches connected in series with the associated freewheeling diodes. A switch is made up of two 75A IGBTs connected in parallel. The upper switch is referred to as TOP IGBT the lower as BOT IGBT. This module uses 1200V Trench 4 IGBTs with an internal 10Ω gate resistor and CAL4 freewheeling diodes. The chip internal gate resistor is needed to avoid parasitic oscillations between parallel IGBTs.

Figure 13: MiniSKiiP®39AC12T4V1

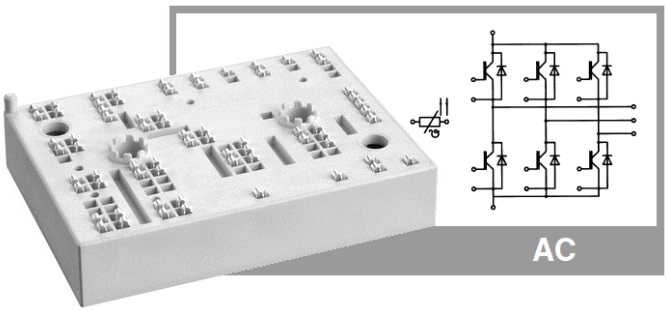

In this test on the MiniSKiiP®39AC12T4V1, as with the MiniSKiiP®24NAB12T4V1, turn-off of the diode D_2 occurs when turning on the complementary IGBT T_1. Figure 14 (left) shows the block diagram of this test setup. Since the chip internal gate-emitter voltage cannot be measured, it was simulated. Figure 15 shows the results of the simulation. 1Ω was used as external gate resistors both for turning on and off of the IGBTs, as shown in the datasheet.

Experience has shown that the effect of the Miller capacitance is the dominant factor influencing the gate circuit for modules with internal gate resistors. For this reason, the influence of the parasitic inductances is not taken into account here.

Figure 14: Measurements on the MiniSKiiP®39AC12T4V1

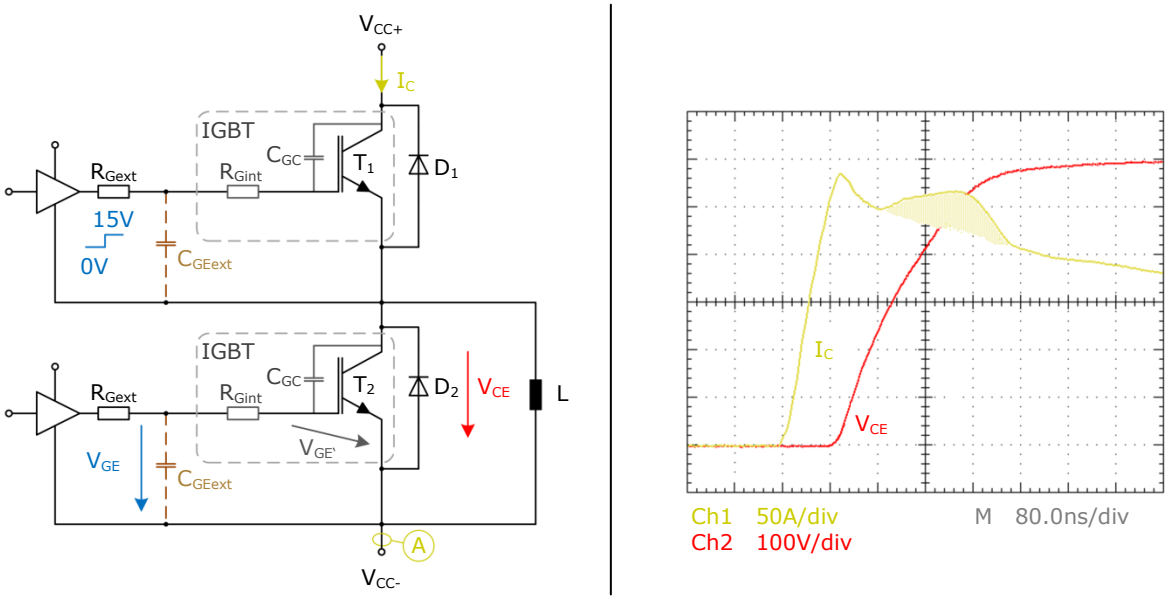

Figure 14 (right) shows the characteristic of the collector current of T_1 and the collector-emitter voltage of IGBT T_2 during the turn-on of IGBT T_1. The collector-emitter voltage of IGBT T_2 is determined by the diode D_2. When the blocking voltage builds up across it the collector-emitter voltage of the IGBT T_2 increases to the same extent.

When the reverse voltage builds up across diode D_2, a displacement current flows in the direction of the gate, due to the Miller capacitance of the IGBT T_2. This raises the gate-emitter voltage and causes the parasitic turn-on of IGBT T_2. A cross current flows from V_{cc+} to V_{cc-} which increases the energy dissipation in IGBT T_1 and IGBT T_2. The parasitic switching of IGBT T_2 is indicated by the shape of the curve of the collector current of IGBT T_1. The shaded area during the decay phase of the diode reverse current indicates the duration of the parasitic turn-on of IGBT T_2.

Figure 15 shows the simulated gate-emitter voltages of IGBT T_2 without external gate-emitter capacitance (left) and with external gate-emitter capacitance (right). The simulation shows that the measurable gate-emitter voltage V_{GE} offers little explanation for what is responsible for the parasitic turn-on, which is the internal gate-emitter voltage $V_{GE'}$. This is due to the ratio of the external gate resistor to the internal gate resistor. Since the same current flows through both resistors, the voltage across the internal gate resistance is significantly larger than the one across the external resistance.

The procedure to use an external gate-emitter capacitance to reduce the effect of the Miller capacitance, as has been demonstrated by the example of the MiniSKiiP®24NAB12T4V1, is not successful with the MiniSKiiP®39AC12T4V1. This is due to the internal gate resistance, where the largest part of the voltage drop occurs, which is caused by the displacement current through the Miller capacitance. In this case, sufficient protection against parasitic switching can only be achieved by a negative gate turn-off voltage of the driver.

Figure 15: Simulation MiniSKiiP®39AC12T4V1

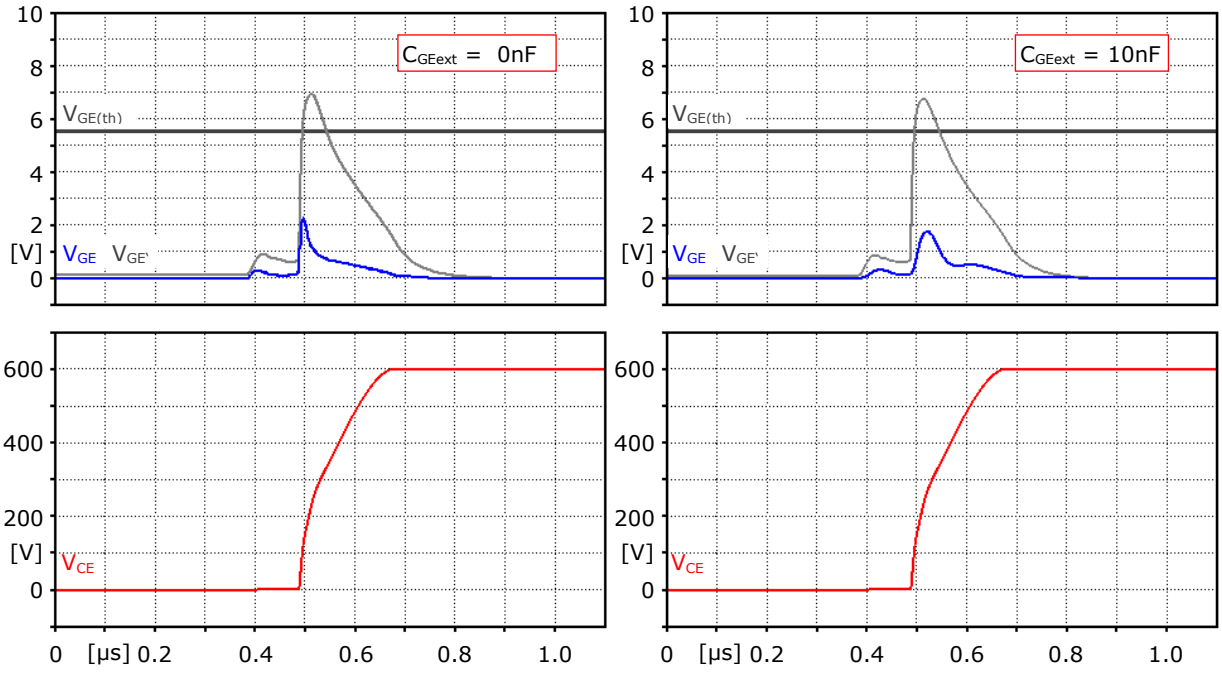

4. Conclusion

Unipolar control of low power modules with 1200V IGBT Trench 4 without internal gate resistors is possible if a few basic rules are observed. The biggest challenge is the connection of the driver, since the gate turn-off voltage is just a few volts below the gate threshold voltage. In order to prevent parasitic switching, a suitable clamping circuit is necessary, to be integrated into the gate circuit. This, as described in this application note, can be realized with the help of an external gate-emitter capacitance, or one of the popular active Miller clamping circuits.

Considering the energy dissipation occurring with unipolar switching of a 1200V IGBT Trench 4, it is proving a great advantage that the turn-off losses are nearly constant over a wide range of gate resistance values. This means that the difference is very low between the energy dissipations in unipolar switching and the energy dissipations in bipolar switching. However, the change in switching times must be observed and a possible adjustment of the interlock times be made.

With increasing power of the modules it will become more difficult to integrate an effective clamping mechanism into the gate circuit, since the influence of the parasitic inductances on the gate-emitter voltage increases.

Modules with IGBTs that have internal gate resistors can not at all, or only insufficiently, be protected by a clamping circuit. This is due to the feedback by the displacement current of the Miller capacitance, which leads to a voltage drop on the internal gate resistance and thus raises the gate-emitter voltage. IGBTs with an internal gate resistor should always be turned off with a sufficiently negative voltage.

Symbols and Terms

Letter Symbol	Term
C	Collector
CAL	Controlled axial lifetime
C_{GC}	Gate-Collector-capacitance (Miller capacitance)
C_{GE}	Gate-Emitter capacitance
C_{GEext}	External Gate-Emitter capacitance
C_{GEint}	Chip internal Gate-Emitter capacitance
D	Diode
$di_{L\sigma}$ / dt	Change of current per unit of time within the parasitic inductance
dv_{CE} / dt	Change of voltage per unit of time of the Collector-Emitter voltage
E	Energy dissipation
E	Emitter
E_{off}	Energy dissipation during turn-off time
E_{on}	Energy dissipation during turn-on time
E_{rr}	Energy dissipation during recovery time (diode)
f_{sw}	Switching frequency
G	Gate
IGBT	Insulated Gate Bipolar Transistor
I_C	Collector current
i_{GC}	Displacement current due to Miller capacitance
$i_{L\sigma}$	Current within the parasitic inductance
L	Load inductance
L_σ	Parasitic inductance
P	Power
P_V	Power loss
R_D	Internal driver resitance
R_G	Gate resistor
$R_{G'}$	Imaginary Gate resitance
R_{Gext}	External Gate resistor
R_{Gint}	Internal Gate resistor
R_{Goff}	Gate resistor (turning off)
R_{Gon}	Gate resistor (turning on)
t	Time

Letter Symbol	Term
T	IGBT
$t_{d(off)}$	Turn-off delay time
$t_{d(on)}$	Turn-on delay time
T_j	Junction temperature
ΔV	Change of voltage
V_{CC}	Supply voltage
V_{CC+}	Positive supply voltage
V_{CC-}	Negative supply voltage
V_{CE}	Collector-Emitter voltage
$V_{G(off)}$	Gate turn-off voltage (driver)
V_{GE}	Gate-Emitter voltage
$V_{GE'}$	Gate-Emitter voltage (chip potential)
$V_{GE(th)}$	Gate-Emitter threshold voltage
$v_{L\sigma}$	Voltage across the parasitic inductance

A detailed explanation of the terms and symbols can be found in the "Application Manual Power Semiconductors" [2]

References

[1] www.SEMIKRON.com
[2] A. Wintrich, U. Nicolai, W. Tursky, T. Reimann, "Application Manual Power Semiconductors", ISLE Verlag 2011, ISBN 978-3-938843-666
[3] M. Hermwille, "IGBT Driver Calculation", Application Note AN-7004, SEMIKRON
[4] M. Hermwille, "IGBT Gate Resistor – Principle and Application", Application Note AN-7003, SEMIKRON

HISTORY

SEMIKRON reserves the right to make changes without further notice herein

DISCLAIMER

SEMIKRON reserves the right to make changes without further notice herein to improve reliability, function or design. Information furnished in this document is believed to be accurate and reliable. However, no representation or warranty is given and no liability is assumed with respect to the accuracy or use of such information, including without limitation, warranties of non-infringement of intellectual property rights of any third party. SEMIKRON does not assume any liability arising out of the application or use of any product or circuit described herein. Furthermore, this technical information may not be considered as an assurance of component characteristics. No warranty or guarantee expressed or implied is made regarding delivery, performance or suitability. This document supersedes and replaces all information previously supplied and may be superseded by updates without further notice.

SEMIKRON products are not authorized for use in life support appliances and systems without the express written approval by SEMIKRON.

SEMIKRON INTERNATIONAL GmbH
P.O. Box 820251 • 90253 Nuremberg • Germany
Tel: +49 911-65 59-234 • Fax: +49 911-65 59-262
sales.skd@semikron.com • www.semikron.com